We are IntechOpen, the world's leading publisher of Open Access books Built by scientists, for scientists

4,800
Open access books available

122,000
International authors and editors

135M
Downloads

Our authors are among the

154
Countries delivered to

TOP 1%
most cited scientists

12.2%
Contributors from top 500 universities

CLARIVATE ANALYTICS BOOK CITATION INDEX INDEXED

WEB OF SCIENCE™

Selection of our books indexed in the Book Citation Index in Web of Science™ Core Collection (BKCI)

Interested in publishing with us?
Contact book.department@intechopen.com

Numbers displayed above are based on latest data collected.
For more information visit www.intechopen.com

18

Hot Chemistry with Cold Molecules

Tapas Goswami and Debabrata Goswami
Department of chemistry, Indian Institute of technology Kanpur, Kanpur-208016, India

1. Introduction

Control of chemical reactions that focuses on the selective cleavage or on the formation of chemical bonds in a polyatomic molecule is a long-sought-after goal for chemists. Attempts have been made since the early days of lasers (1960) to make this dream come true (Rousseau, 1966). In most of the experiments, selectivity is lost because of the rapid intramolecular vibrational energy redistribution (IVR) which occurs on picosecond time scales. This simply leads to heated molecules. Supersonic molecular beam techniques have proven to be an excellent method for producing isolated cold molecules in the gas phase, where the molecules are in their lowest rotational and vibrational states and as a result several relaxation rates like the collisional and the IVR rates are much slower (Smalley et al., 1977; Levy, 1981). By combining ultrafast laser technology with supersonic molecular beam technique in a novel way, several control schemes known as 'coherent control', have been proposed that make use of the coherent nature of laser radiation (Zewail, 1980; Bloembergen & Zewail, 1984). Furthermore, study of control is typically pursued in molecular beams in order to isolate the elementary processes to be studied from surrounding solvent perturbations.

In a chemistry laboratory, however, the conventional control that we generally use in increasing the yield of the desired products in the chemical synthesis are macroscopic variables, such as, the temperature, pressure, concentration, etc. Sometimes catalysts are also used to control the chemical reactions. But the methods involved in this type of conventional cases are based on the incoherent collision between collision and we cannot get direct access to the quantum mechanical reaction pathway. On the other hand, in the quantum control of chemical reactions, molecular dynamics involved can be altered by specifically designed external light fields with different control parameters, namely, the intensity, phase, frequency, and polarization, which can vary with time. Using such methods, one can reach a user-defined chemical reaction channel more selectively and efficiently (Brixner & Gerber, 2003). The short temporal duration of ultrafast laser pulses results in a very broad spectrum (Fig.1). The output of our amplified laser system has pulse duration around 50 femtosecond and spectral bandwidth of around 18 nm. Possibilities of manipulating such an ultrafast coherent broadband laser pulses have brought forth the exciting field of ultrafast pulse shaping. Pulse shaping involves the control over amplitude, phase, frequency, and or inter-pulse separation (Goswami, 2003). Control of chemical reactions by laser can have various applications in diverse industrial and biological or

medicinal settings e.g. microelectronic lithography, the fabrication of gene chips, and photodynamic therapy (Levis et al., 2001). Even in quantum information processing, controllability of the quantum system is the key issue (Ahn et al., 2000; Vivie-Riedle & Troppmann, 2007). All these probable applications of coherent control have made this a very 'hot' research area in chemistry and physics.

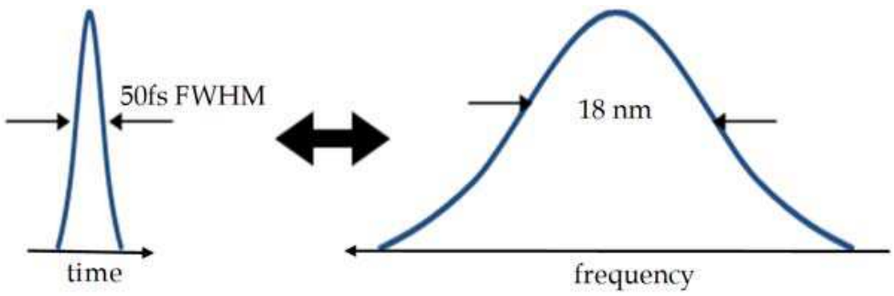

Fig. 1. An ultrafast laser pulse in time and frequency.

To begin with coherent control studies, it is essential to choose a simple atomic or molecular system, whose characteristics are fully known and can be understood very simply, such that we can easily analyze our results. We also need to have an easy detection system. Thus, the first and foremost objective is to design and build, for instance, a supersonic molecular beam chamber with linear time of flight mass spectrometer to produce an isolated cold molecular beam whose mass spectra can be detected.

Coincidentally, this year 2010 is considered as the hundred years of invention of molecular beam technique (Herschbach, 1987). Molecular beam is a large number of molecules in laminar flow, i.e., moving in straight and almost parallel trajectories in a practically collision free environment in a highly evacuated space. One of the essential elements in producing the molecular beam is the high vacuum pump. High vacuum pump was invented almost hundred years ago in the year 1910. Molecular beam study was started just after the invention of the high vacuum pump.

The control over the fragmentation and chemical reactions using shaped ultrafast laser pulses was demonstrated by different schemes of experiments by various groups of scientists (Assion et al., 1998; Levis et al., 2001; Daniel et al., 2001; Levis et al., 2002; Brixner et al., 2003; Daniel et al., 2003). All of their experiments are based on the closed loop approach using learning algorithms to control the laser field with feedback from the experimental signal. The resultant pulse shapes obtained by an adaptive approach were not always found to be a globally optimized solution (Assion et al., 1998; Levis et al., 2001; Weinacht et al., 1999; Itakura et al., 2003). Furthermore, the physical significance of such complex shaped pulses to the actual processes leading to discrimination among the fragmentation channels and their mechanisms are often too difficult to apprehend limiting the generalization of such feedback schemes. A continued effort, therefore, exists on the control of such fragmentation process from simpler pulse modulation concepts.

One of the easiest pulse modulation schemes is frequency chirping. Chirping essentially refers to the process of arranging the frequency components in a laser pulse with certain phase ordering. Linear ordering can be easily achieved by dispersing the ultrafast pulses through a pair of gratings. This ordering of frequency components results in the lengthening of an otherwise bandwidth limited ultrafast laser pulse. For positively chirped pulse leading edge of the pulse is red shifted and the trailing edge is blue shifted with respect to the

central frequency of the pulse. Negative chirp corresponds to the opposite effect. The first experimental demonstration of control using simple linear chirped laser pulses was by Warren and co-workers in the early 1990s (Melinger et al., 1992). Subsequently, several experimental and theoretical developments have made linear chirped pulse control a very attractive field of research (Krause et al., 1993; Cerullo et al., 1996; Pestrik et al., 1998; Yakovlev et al., 1998; Cao et al., 1998). Control of fragmentation with simple linear chirped pulses as a control scheme has also become an active field of research in recent years.
In this chapter on 'hot' chemistry with 'cold' molecules, we first present our experimental scheme of producing the 'cold' molecules in the supersonic beam chamber followed by the laser schemes to induce 'hot' chemistry. The resulting chemistry ensuing from such technological developments are discussed in the subsequent sections.

2. Experimental

Design of our molecular beam setup:
An engineering drawing of the system was prepared using AUTOCAD software (Fig.2). The design of our molecular beam setup (Fig.2) consists of three chambers with differentially pumping by turbo pumps. The three chambers were designed to attain a supersonic molecular beam region (source chamber), a laser interaction region (Fig.3) and a mass detection region. Each of the chambers is connected to turbo molecular pumps which are in

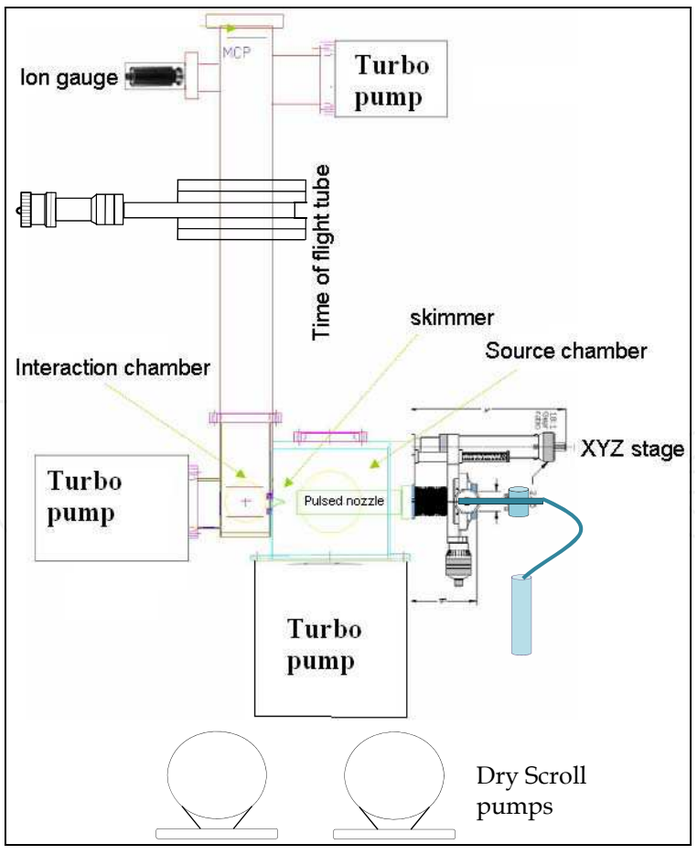

Fig. 2. Diagram of our Molecular beam chamber setup.

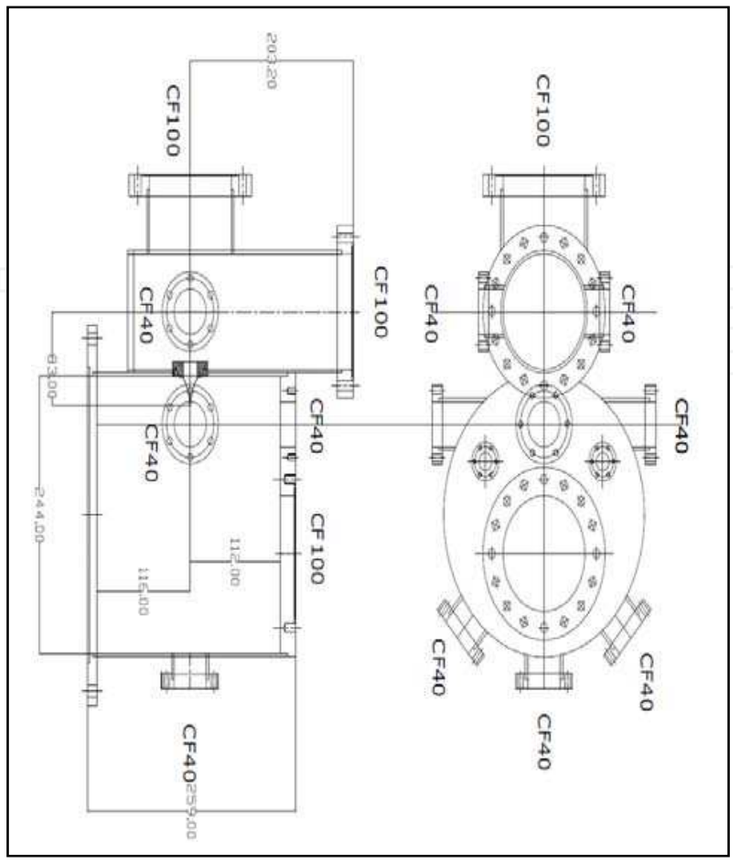

Fig. 3. Autocad diagram of the source and part of the interaction chamber. The flanges are also marked with their sizes. Diagram on top is the top view of the chamber what was designed and fabricated. Diagram in the bottom is the side view of the chamber with all viewports. CF- conflate flat copper gasket flange.

turn connected to dry scroll pump. Vacuum chambers were fabricated based on our design and requirements for complete oil free systems using SS-304 stainless steel and conflate connections. Design of our particular single beam experiments depends mainly on the considerations of signal-to-background noise ratio. The size and geometry was chosen to match the pulse duration of the source and the detector geometry. The chamber geometry suggests that a cylinder or cube with height and width approximately equal and with the beam source located so that the nozzle is about equal distance from the walls ahead and the sides of the beam.

It is sometimes advantageous in pumping speed requirement when the molecular beam source is kept directly into the throat of the vacuum pump. Because most high speed pumps are designed for mounting at the bottom of the chamber, this configuration implies mounting the molecular beam source directly above the pump. The source chamber or the supersonic molecular beam region is larger and it has the dimension of 10.19 inch (259 mm) height and 9.6 inch (244 mm) diameter. Source chamber is pumped by a turbo molecular pump (Varian Turbo V2K-G) which has a 2000 l/s pumping speed. The 2000 l/s turbo pump is connected to the source chamber with ISO250 F flange. This turbo pump is connected to the Dry scroll pump (Varian DS600) via stainless steel hose with a KF40 flange.

The source chamber contains a pulsed valve with 0.5 mm nozzle attached (Series 9 General valve) and a 1mm skimmer which is the only opening into the interaction chamber and it allows only the central portion of the expanded molecular beam. The pulsed valve is mounted on a compact X-Y-Z translation stage from MDC Inc. The Series 9 pulsed valve (General Valve, Inc.) provides a versatile way of introducing high backing pressures of gas into vacuum. The series 9 valve comes with its own Iota One pulser, which can be triggered either internally or externally (used in the experiments described in this chapter) and then be pulsed for a defined width. The valve consists of a magnetically actuated poppet and spring mechanism which requires sufficient rise time for opening and closing (250 μs each half cycle, which limits its maximum repetition rate to 35 Hz). We keep the repetition rate of the pulsed valve at 10 Hz and the pulse duration at 100 μs for the experiments described here. A poppet of tip size matched with the orifice (diameter 0.5 mm) of the nozzle is fitted inside the armature by a compressed stainless steel spring to close the orifice. The Iota One pulser generates a brief high voltage of 275-295 V and it pulls the armature with the tip to open the orifice and then the voltage drops to a 28 V holding voltage for the remainder of the pulse. To get the full benefit of a pulsed molecular beam, it is essential to have a leak tight pulsed valve. We used a PEEK (polyether-ketone resin) poppet material which can deform within few hours of use and needed to be replaced regularly. A leaking poppet will increase the foreline pressure on the roughing pump thermocouple gauge and a strong degradation of any type of collected ion signal and often large fluctuations in the ion gauge readings of source chamber pressure. For the electrical connection to the pulsed valve there is CF40 electrical feed through flange in the source chamber.

Our sample chamber is kept outside the vacuum chamber and is connected to the pulsed valve with a 0.5 inch diameter and 12 inch long stainless steel tube. The tube passes through the back flange of the source chamber with a conflate connection and is connected to the He gas supply cylinder.

The nickel skimmer of 1 mm diameter is used to separate the source chamber from the interaction chamber and it allows only the cold core of the supersonic molecular beam. The skimmer is a cone with a base diameter of 27.9 mm, an orifice diameter of 1mm and a length of 25.4 mm. It has a 2.5 mm clamping edge. Skimmers have ultra-thin walls and ultra-sharp orifice edges to minimize the skimmer interference with molecular beam.

The interaction chamber is pumped by a 500 l/s turbo molecular pump (TurboV-550). Turbo V-550 pump is connected to the chamber with CF100 conflat flange. It contains two sapphire view port (CF40) to pass the laser beam through the interaction region where the electric plates for the time of flight mass spectrometer is situated.

Fragment ion detection chamber with flight tube is pumped by a 300 l/s turbo pump (TurboV-300) and the pump is kept near the 18 mm dual MCP detector. The MCP detector is separated by a gate valve, when the experiment is not in operation, such that we can always maintain low pressure in the detection chamber. Other element in the detection chamber is the time of flight mass spectrometer, which will be described below.

Vacuum pressure is monitored in both source and detection chamber by Bayard-Alpert ionization gauge detector and convector gauge. After baking the vacuum chambers, we are able to obtain base pressure of around 10^{-8}torr and 10^{-9}torr in the source and interaction chamber respectively. The pumping speed of our turbo pumps are sufficient enough to maintain a chamber pressure of 10^{-6}torr and 10^{-7}torr, respectively, in the source and the interaction chamber, when the nozzle is in operation at 10 Hz repetition rate for a backing pressure of 2-3 atmosphere of He.

Our time of flight mass spectrometer:
Our time of flight tube (Fig. 4) was manufactured by R. M. Jordan Co. (C-677 lens stack assembly) according to our particular requirements. A skimmed (0.040 inch dia.) supersonic molecular beam is directed through the space (1 cm) between two plates and is ionized by a laser beam which intersects it at right angles. The ions thus created are repelled by the repeller plate (VA1 =+4100 Volts) and drawn through the extraction Grid (VA2 = +3500Volts). They are then accelerated through the Ground Grid (VA3) into the Flight tube. Total length of the drift tube is 56 inch from laser centerline to the detector.

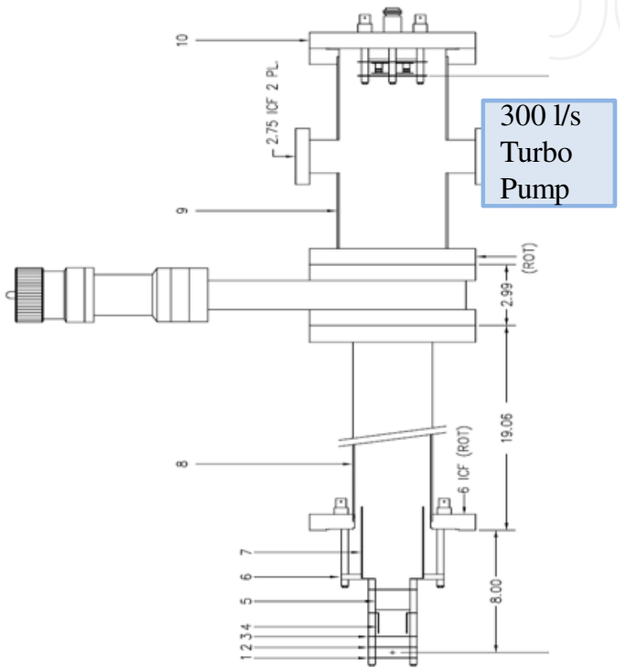

Fig. 4. Design of our Time of Flight tube with a manual Gate valve, 1. Repeller plate VA1. 2. Extraction grid VA2. 3. Acceleration grid GND. 4. X steering plates VX1, VX2. 5. Y steering plates VY1, VY2. 6. Mounting ring. 8. Flight tube 2.875" diam. 9. Side-port Tee. 10. C 16MM dual MCP detector. All measurements are shown in inches.

During this transit the ions pass through the Einsel lenses (no power supply is provided) and between the deflection plates VX1=+157 Volts, VX2=+176 Volts, VY1= -45 Volts, VY2= -21Volts. These plates steer the beam on to the repeller and Detector Grid and compensate for the transverse displacement due to any initial molecular beam velocity vector.
When each of these ions arrives at the detector it will impact the first microchannel plate (VD1= -2200 Volts) with about 6000 volts of energy. This impact will deliver approximately 104 electrons onto the face of the second microchannel plate (VD2=-1200 Volts). Each of these secondary electrons will generate another 104 electrons in the second plate. These electrons exit the bottom of the plate (VD3= -200Volts) and accelerate the final 200 Volts to the 50 Ohm anode which is at ground potential.
The MCP plates (Burle Electro-optics) are discs of lead glass ~0.75 mm thick and 5.2 cm^2 in diameter. (Fig. 5) It consists of around 106 cylindrical channels with a diameter of 10μm and an inter-channel separation of 12μm. Electrons emitted from the channel walls by ion impact are accelerated toward the other side of the plate by a differential electric field. Secondary

ion emission from the channel walls initiates an electron avalanche which is collected by an anode and then output through a 50 Ohm termination circuit to an oscilloscope for observation. To increase MCP gain, additional MCPs can be placed in series. We used a 2 plate MCP stack with a total gain of 10^6 and a sub-nanosecond rise time. A grid on front of the MCP stack is held at ground potential to allow a field free drift region for ions in the flight tube. The cylindrical symmetric flight tube can be biased to a few hundred volts but it is usually held at ground. In order to protect the MCP against sparks causing short circuit, the pressure has always been kept below 10^{-5} torr. The minimal pressures in the TOF and source chamber were kept about 10^{-7} and 10^{-6} torr.

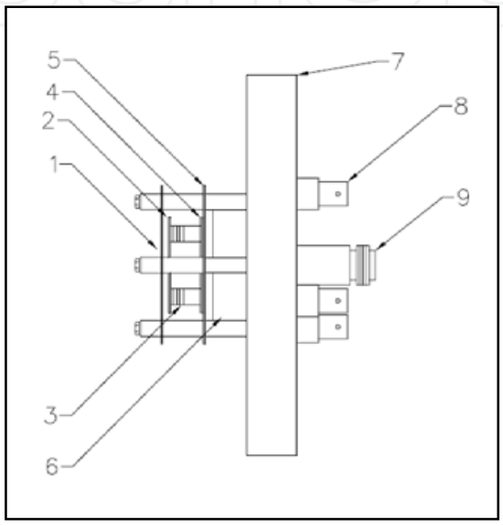

Fig. 5. Design of our microchannel plate detector on a conflate flange: 1- Input grid, 2-spring cap, 3-spring, 4-microchannel plate stack assembly, 5- base plate, 6- anode shield, 7- detector flange assembly, 9- 50Ω feedthrough.

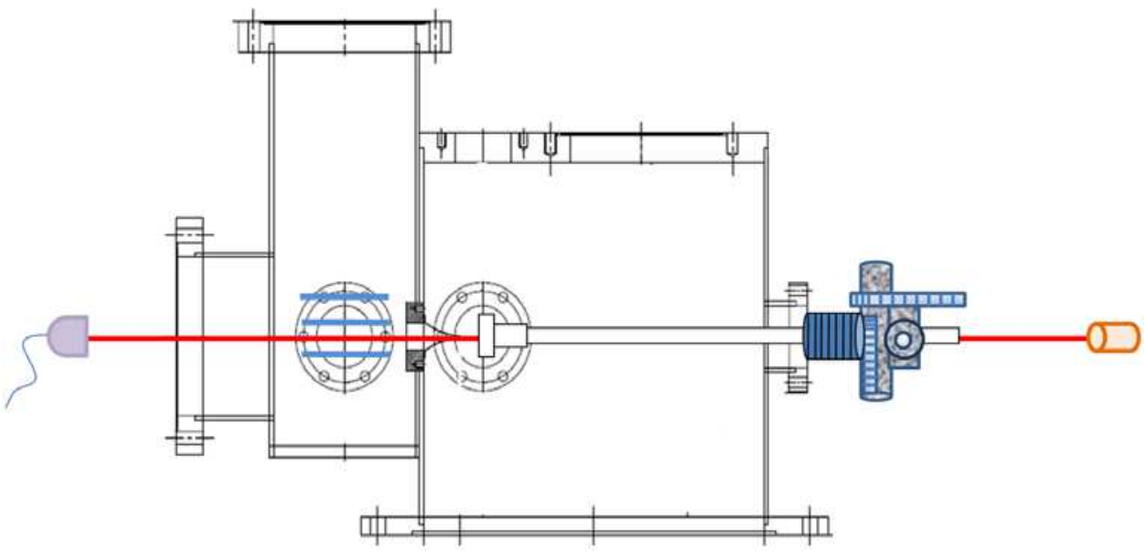

Fig. 6. Alignment of nozzle, skimmer and centre of the repeller and extraction plate.

Alignment of the nozzle, skimmer, and the centre of the repeller and extraction plates was achieved by aligning using a laser pointer with the pulsed valve's internal part removed and also with the turbo pump near the interaction region removed.(Fig. 6) The XYZ position of the pulsed valve mounting assembly was adjusted using the XYZ mount (MDC Vacuum Inc.) so that its centre falls in the line of the skimmer and the centre of the two plates (Repeller and Extraction). Slight adjustment of the position of the skimmer to pass the beam into the centre of the two electrical plates was done.

Data Acquisition:

Synchronization of 1 kHz, 50fs pulsed laser with 10 Hz, 100µs pulsed molecular beam was done by a homemade delay generator.(Fig. 7) Our delay generator can give a delay upto ~2 ms. We take the master clock of 1 kHz from our pockel cell and used as an external trigger for the delay generator and the delay generator is used to first count down the frequency from 1 kHz to 10 Hz and then delay it as per necessity to get the stable time of flight spectra. 10 Hz delay out is used to trigger the pulsed valve and the 10 Hz TTL out is used to trigger the MCP signal in Oscilloscope. Data acquisition procedure is shown pictorially in Fig. 8. Here we give the delay to the pulsed molecular beam by around 800 µs to make it synchronize with the next 1 kHz femtosecond laser pulse. TOF signal was collected using 1GHz digital oscilloscope. Each data was averaged with 500 laser shots. Fig. 9 is the picture of our setup.

Calibration of our linear time of flight mass spectrometer:

Calibration of our time of flight mass spectrometer was done by taking the mass spectra of some sample whose mass spectra is reported, then m/z vs t^2 was plotted and after fitting it linearly according to the equation $m/z=At^2+B$, we can find the calibration parameter A and B. For unknown sample we can easily convert flight time to m/z following the above equation where A and B are known. In our case, after fitting linearly according to the equation mentioned above we get calibration parameter A= -216.9 and B= 0.68. (Fig. 10) Mass spectra of n-propyl benzene was calibrated using the above calibration parameter and shown in Fig. 11.

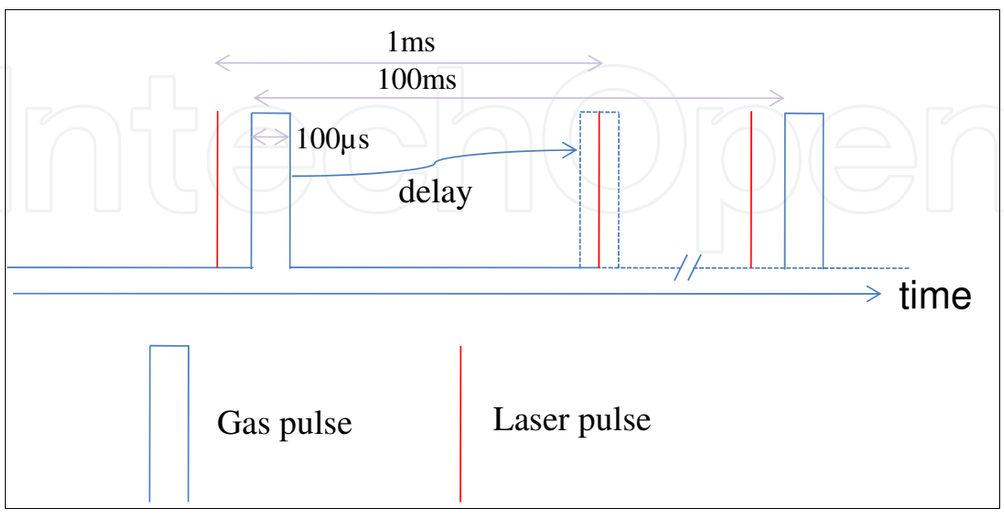

Fig. 7. Synchronization of pulsed molecular beam and laser pulses.

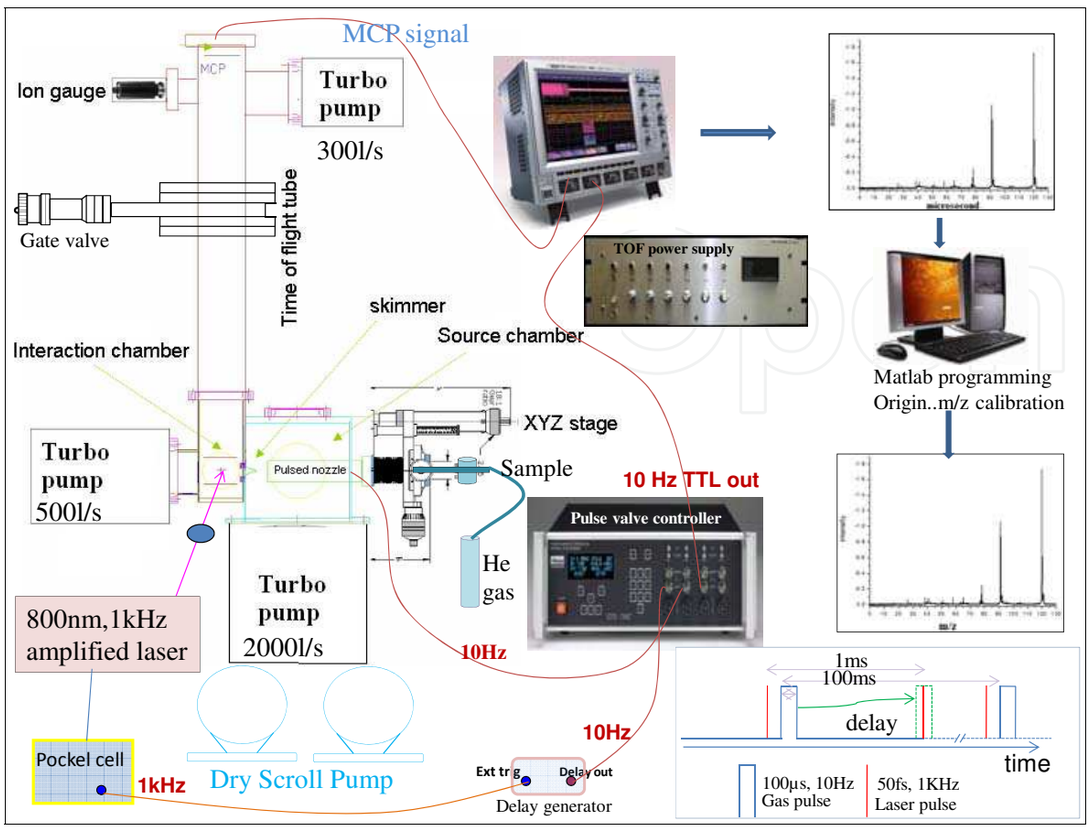

Fig. 8. Complete experimental setup for data acquisition.

Fig. 9. Picture of our supersonic molecular beam linear time of flight mass spectrometer.

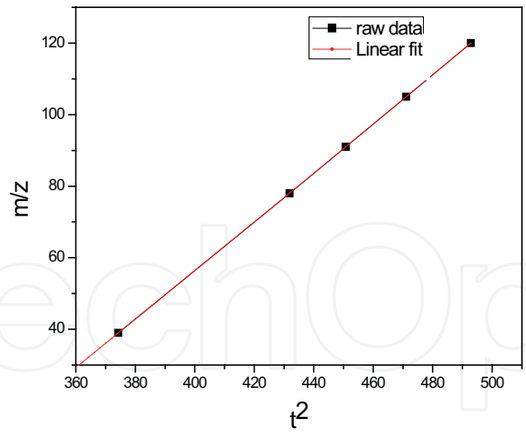

Fig. 10. Calibration line and its linear fit.

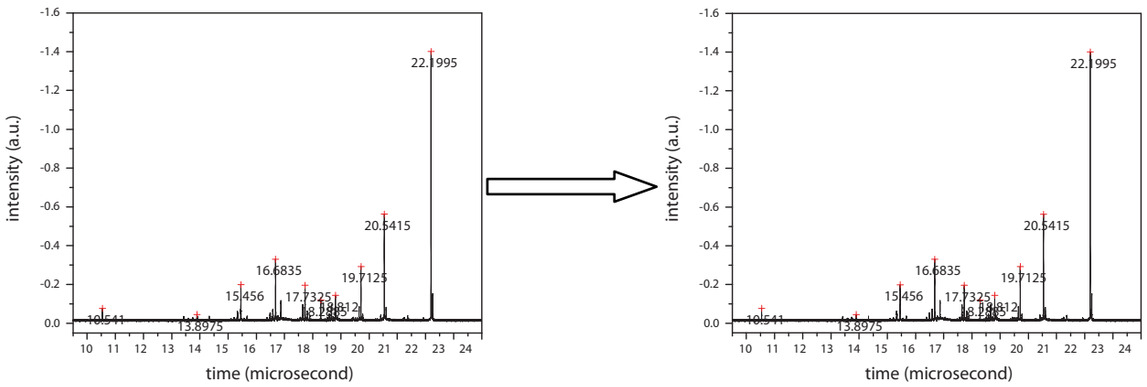

Fig. 11. Calibration of mass spectra of n-propyl benzene.

In mass spectrometry it is conventional to measure resolving power by the ratio of m/Δm where Δm is a discernable mass difference. In TOFMS it is convenient to work in the time domain (Guilhaus, 1995; Opsal et al. 1985). Thus the resolving power m/Δm can be measured in terms of t/Δt as follows:

Since $m \propto t^2$, $m=At^2$, and $dm/dt=2At$ where A is constant;

$$dm/m=2dt/t$$

$$\text{Thus } m/\Delta m=t/2\Delta t$$

The finite time interval Δt, is usually the full width at half maximum (height) of the peak (FWHM).

Laser System:

The Laser system used in this experiment is a Ti:Sapphire multipass amplifier (Odin, Quantronix Inc.), which operates at 800 nm with 50 fs FWHM pulses at 1 kHz with energy of ~1 mJ. It is seeded with a homebuilt Ti:Sapphire Oscillator (starting point: K&M Labs Inc. oscillator kit). The oscillator is pumped by a Nd:YVO4 (Verdi 5, Coherent Inc.), resulting in femtosecond pulses with a centre wavelength of 800 nm and a spectral bandwidth of 50 nm FWHM at 94 MHz repetition rate and an average power of 400 mW. The oscillator output is stretched and then fed into the Ti:Sapphire multipass amplifier which is pumped by the

second harmonic of Nd:YAG laser operating at a repetition rate of 1 kHz (Corona, Coherent Inc.). The chirped ultrafast laser pulses can be easily produced from our suitably modified compressor setup for the amplified laser system. As we increase the spacing between the compressor gratings relative to the optimum position for minimum pulse duration of 50 fs, we generate a negatively chirped pulse. Conversely, we obtain the positively chirped pulse by decreasing the inter-grating distance. Pulse durations were measured using a home-made intensity auto-correlation for the transform-limited pulse, as well as for the various negatively chirped and positively chirped pulses (Fig. 12). The pulses were further characterized by second harmonic frequency resolved optical gating (SHG-FROG) technique. Fig. 13a shows a typical SHG-FROG trace of our near transform-limited pulse that was collected using GRENOUILLE (Swamp Optics Inc.). In Fig. 13b retrieved spectra and phase of the transform limited pulse is shown. From this Fig. 13b is found that phase of the laser pulse is constant within the bandwidth of the laser pulse and hence it is made sure that at optimal grating distances we get the shorter pulse which is transform limited. In Fig. 14a, we show the SHG spectrum of the of the transform limited pulses after frequency doubling with 50 μm type-1 BBO crystals as well as the spectrum of the transform-limited pulse collected with a HR-2000 spectrometer (Ocean Optics Inc.). From the Fig. 14b, FWHM of the near transform limited pulse is found to be ~18 nm. The minimum time duration of a transform limited pulse giving a spectrum with $\Delta\lambda$ (18 nm) at FWHM, central wavelength (800 nm) and the speed of light (m/s) c: $\Delta t = K\frac{\lambda_0^2}{\Delta\lambda \cdot c}$ where K is the time-bandwidth product (K=0.441 for Gaussian pulse), Δt is found to be 50 fs for 18 nm bandwidth pulse which is our transform limited pulse.

The laser pulses are then focused with a lens (focal length = 50 cm) on a supersonically expanded molecular beam of n-propyl benzene at the centre of a time of flight chamber. The polarization of the laser was horizontal as it enters the mass spectrometer and is perpendicular to ion collection optics. The Mass spectra from our particular beam chamber constructed with dry-scroll pumps and turbo-molecular pump as described above has the advantage that it does not contain any extraneous water and hydrocarbon peaks and thus has better sensitivity for organic samples as reported here.

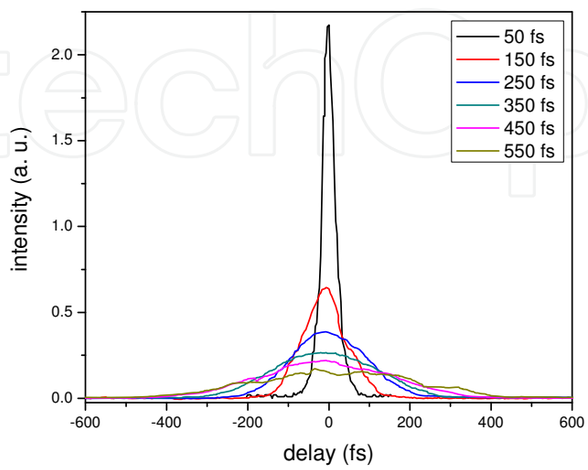

Fig. 12. The various autocorrelation traces of the pulse for different chirps.

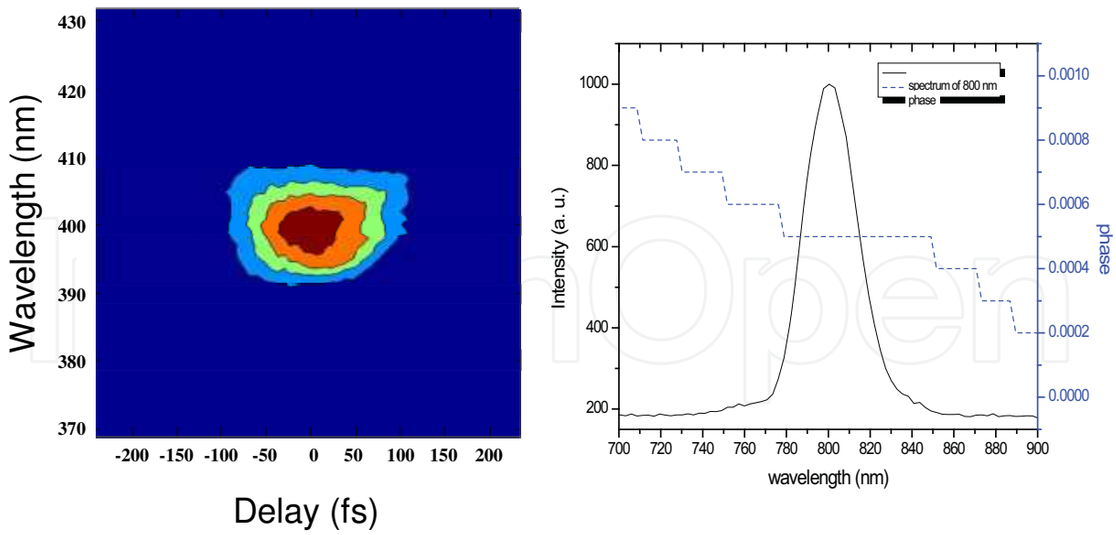

(a) (b)

Fig. 13. (a) SHG-FROG trace of our near transform limited 50 fs pulse, (b) retrived spectra and phase of the transform limited pulse.

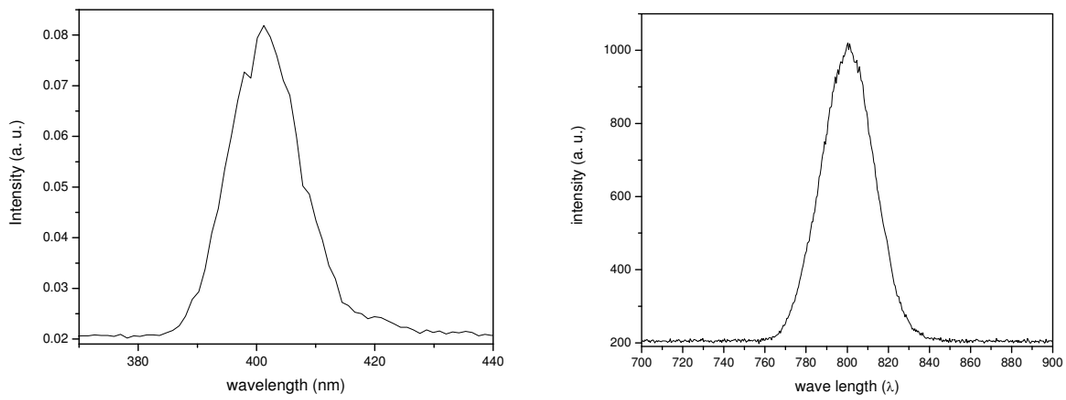

Fig. 14. (a) SHG Spectrum of transform limited pulse, (b) spectrum of the transform limited pulse.

Generation of Femtosecond chirped pulses:

Femtosecond chirped pulse can be easily generated by the compressor setup. This pulse increases its frequency linearly in time (from red to blue). In analogy to bird sound this pulse is called a "chirped" pulse. Our compressor setup (Fig. 15) consists of a pair of grating and a high reflective mirror. Our compressor gratings have 600 grooves/mm (Newport), and have throughput efficiency of 60%. One of the gratings is placed on a translation stage. By changing the distances between the two gratings and carefully aligning the optical paths at some optimal position a shorter near transform limited 50 fs laser pulse is generated. The transform limited condition is confirmed by characterizing the laser pulses at transform limited condition by measuring the SHG-Frog and autocorrelation trace. As we increase the spacing between the two gratings relative to the optimum position we can generate negatively chirped pulse. Conversely if we decrease the inter-grating distance we can generate positively chirped pulse.

An incident laser pulse of spectrum E_0 (ω) will be shaped by the compressor setup and spectrum of the output will be E_0 (ω)$e^{iφω}$. For a light pulse which is centered around $ω_0$ having a reasonably small bandwidth, the total phase can be expanded around $ω_0$ to second order in ω:

$$\varphi(\omega) \approx \varphi(\omega_0) + \frac{1}{1!}\frac{\partial\varphi}{\partial\omega}\Big|_{\omega=\omega_0}(\omega-\omega_0) + \frac{1}{2!}\frac{\partial^2\varphi}{\partial\omega^2}\Big|_{\omega=\omega_0}(\omega-\omega_0)^2$$

Here, the second order term is responsible for group velocity dispersion. In fact, $\beta = \frac{\partial^2\varphi}{\partial\omega^2}\Big|_{\omega=\omega_0}$ is linear chirp coefficient (chirp parameter in the frequency domain) introduced by the compressor and is defined as second derivative of the spectral phase at the center frequency. The linear chirp coefficient (β) can be calculated using the equation:

$$\tau^2 = \tau_0^2 + \left[\frac{4\beta\ln 2}{\tau_0}\right]^2$$

where τ is the pulse duration of the chirped laser pulse and τ_0 is the chirp-free pulse duration of the transform limited pulse in FWHM. Pulse durations were measured by intensity autocorrelation technique. The experimental error in the chirp value calculated from the equation mentioned above is about ±9%.

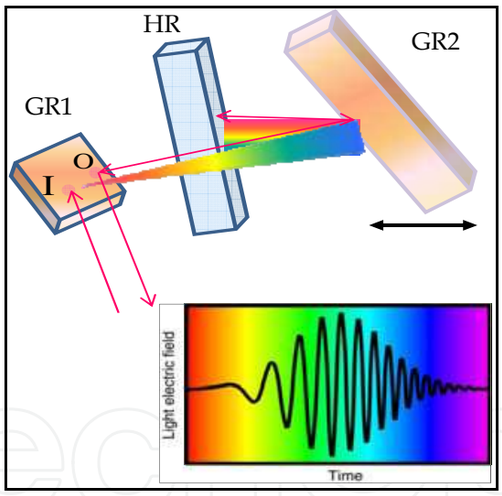

Fig. 15. Compressor setup, GR1, GR2- Garting, HR-high reflective mirror.

3. Results and discussions

Our TOF design provides high resolution when it is used in conjunction with our skimmed supersonic molecular beam chamber. Fig. 16 shows the time of flight mass peak of n-propyl beanzene cation. This was taken using femtosecond laser photo-ionization at 800 nm. The resolution is defined as R = t/(2Δt), where t is the total flight time of the ion packet and Δt is the FWHM of the peak. In the case n-propyl benzene cation resolution R is found to be around 1113. (Fig. 16) With careful adjustment of the voltages of the time of flight power supply and nozzle to skimmer distance to prevent turbulence on the skimmer, we have

observed ion packet widths of ~10 ns. Resolution R = t/2Δt = 22.1995/(2×0.0097) = 1113, our mass spectra can resolve the adjacent mass peaks in the range of m/z from 0 to 1113 amu.

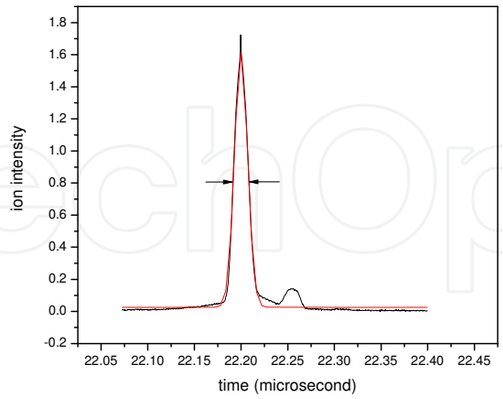

Fig. 16. Ion peak of n-propyl benzene cation

It has been known that the fragmentation processes in polyatomic molecules induced by an intense ultrafast laser field can sometimes exhibit sensitive dependence on the instantaneous phase characteristics of the laser field (Itakura et al., 2003; Pestrik et al., 1998; Mathur & Rajgara, 2003; Lozovoy et al., 2008, Goswami et al., 2009). Depending on the change in sign the chirped laser pulses, fragmentation could be either enhanced or suppressed. Controlling the outcome of such laser induced molecular fragmentation with chirped femtosecond laser pulses has brought forth a number of experimental and theoretical effects in the recent years. However, efforts are continuing for a specific fragment channel enhancement, which is difficult since it also is a function of the molecular system under study. Here we report the observation of a coherently enhanced fragmentation pathway of n-propyl benzene, which seems to have such specific fragmentation channel available. We found that for n-propyl benzene, the relative yield of $C_3H_3^+$ is extremely sensitive to the phase of the laser pulse as compared to any of the other possible channels. In fact, there is almost an order of magnitude enhancement in the yield of $C_3H_3^+$ when negatively chirped pulses are used, while there is no effect with the positive chirp. Moreover, the relative yield of all the other heavier fragment ions resulting from interaction of the strong field with the molecule is not sensitive to the sign of the chirp, within the noise level.

Study of aromatic hydrocarbons has indicated different fragmentation channels (DeWitt et al., 1997). A systematic study of aromatic compounds with increasing chain-length of substituent alkyl groups has indicated that the fragmentation process is enhanced as the chain-length of the alkyl substituent on the benzene ring increases. We have chosen to apply chirped pulse fragmentation control on certain members of these systematically studied aromatic compounds. In general, as reported previously for benzene and toluene, p-nitro toluene, we also find that chirping favors the formation of smaller fragments as compared to the heavier ones. However, n-propyl benzene has the unique property of enhancing a particular fragmentation channel under the effect of chirp.

We record the TOF mass spectra (Fig. 17) of n-propyl benzene using linearly chirped and unchirped ultrafast laser pulses with constant average energy of ~200 mW. Next, we compared the corresponding peaks in mass spectra by calculating their respective integrals

under the peaks and normalizing them with respect to the molecular ion. These results also conform to the case when we just compare the simple heights of the individual peaks. When the linear chirp of the laser pulse is negative, the relative yields of the smaller fragment ion, such as, $C_3H_3^+$ (mass to charge ratio, i.e., m/z = 39) is largely different from those obtained using transform-limited pulses or from the positively chirped pulses, as reflected in the Fig. . The relative yield of $C_3H_3^+$ reaches maximum when the linear chirp coefficient (β, calculated by using the equation as mention earlier) is -8064 fs² and pulse duration is of 450 fs. We would like to point out that the fragment ion $C_6H_5^+$ (m/z = 77) yield is more when the chirp is positive (β=+6246fs²), and this can be attributed to a different fragmentation pathway (Fig.18). However, the observation of enhancement for only one chirp sign implies that the observed enhancements are not due to the pulse width effects, they rather depend on the magnitude and sign of the chirp. Hence coherence of the laser field plays an important role in this photofragmentaion process. It is also seen that relative yields of the heavier fragments like $C_7H_7^+$ (m/z = 91) is not affected by the sign of the chirp.

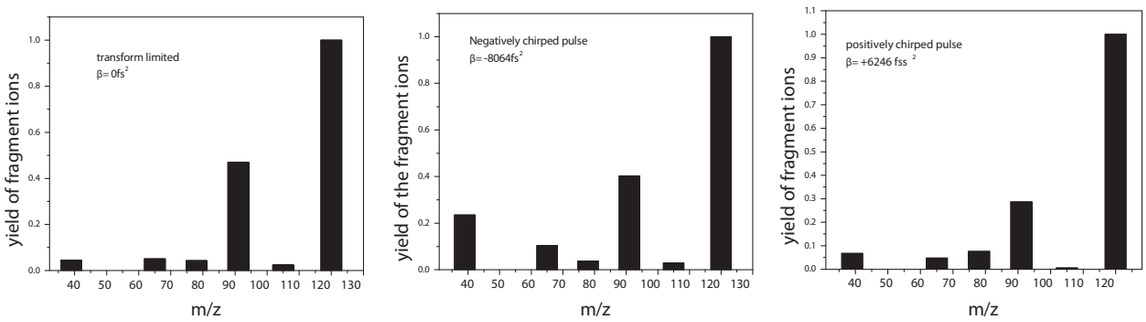

Fig. 17. Effect of chirping on mass spectra of n-propyl benzene, (a) β=0 fs², (b) β=-8064 fs², (c) β=+6246 fs².

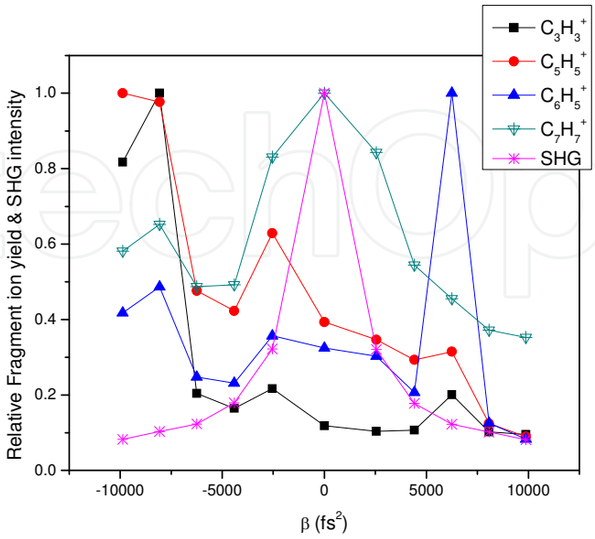

Fig. 18. Effect of chirping the laser pulse on the relative yield of different fragment ions shown in comparison to the integrated SHG intensity at the respective chirps.

The relative yield of $C_7H_7^+$ decreased in both the directions of the chirp and is at its maximum when the pulse is transform limited, indicating that the fragment yield only depends on the laser peak intensity as dictated by its pulse width. We have also seen that the integrated SHG intensity at different chirp is symmetrically decaying around 0 fs^2 (Fig. 18), which confirms that there is nothing systematic in the laser pulse causing the enhancements in the fragmentation process.

4. Conclusions

We have built a molecular beam chamber with linear time of flight mass spectrometer, which can be combined with femtosecond laser in a novel way to study the femtosecond coherent control of supersonically cooled molecules. Our system is constructed with dryscroll pumps and turbo-pumps and is completely free from oil, which is very necessary for any femtosecond laser laboratory. In fact, this oil-free capability ensures that the obtained mass spectra is free from extraneous hydrocarbon peaks, which, in turn, makes our system better sensitive in studying coherent control of organic samples as reported in this book chapter.

We have demonstrated that the phase characteristics of the femtosecond laser pulse play a very important role in the laser induced fragmentation of polyatomic molecules like n-propyl benzene. The use of chirped pulse leads to sufficient differences in the fragmentation pattern of n-propyl benzene, so that it is possible to control a particular fragmentation channel with chirped pulses. Overall, as compared to the transform-limited pulse, negatively chirped pulses enhance the relative yield of $C_3H_3^+$, $C_5H_5^+$, while the relative yield of $C_6H_5^+$ increases in case of positively chirped pulse. In fact, for the $C_3H_3^+$ fragment, the enhancement is almost 6 times for the negatively chirped pulse (β = -8064 fs^2) as compared to that of the transform-limited pulse.

5. References

Rousseau, D. L. J. (1966). Laser chemistry, *Chem. Educ.,* 43, 566-570.

Smalley, R. E.; Wharton, L.; Levy, D. H. (1977). Molecular optical spectroscopy with supersonic beams and jets, *Acc. Chem. Res.*, 10, 139-145.

Levy, D. H. (1981). The spectroscopy of very cold gases, *Science*, 214, 263-269.

Zewail, A. H. (1980). Laser Selective Chemistry: Is It Possible? *Phys. Today*, 33, 27.

Bloembergen, N.; Zewail, A. H. (1984). Energy redistribution in isolated molecules and the question of mode-selective laser chemistry revisited. New experiments on the dynamics of collisionless energy redistribution in molecules possibilities for laser-selective chemistry with subpicosecond pulses, *J. Phys. Chem.*, 88, 5459-5465.

Brixner, T.; Gerber, G. (2003). Quantum control of gas-phase and liquid-phase femtochemistry, *ChemPhysChem*, 4, 418-438.

Goswami, D. (2003). Optical pulse shaping approaches to coherent control, *Phys. Rep.*, 374, 385-481.

Levis, R. J.; Menkir, G. M.; Rabitz, H. (2001). Selective Bond Dissociation and Rearrangement with Optimally Tailored, Strong-Field Laser Pulses, *Science*, 292, 709-713.

Ahn, J.; Weinacht, T. C.; Bucksbaum, P. H. (2000). Information Storage and Retrieval Through Quantum Phase, *Science*, 287, 463-465.

Vivie-Riedle, R. de; Troppmann, U. (2007). Femtosecond Lasers for Quantum Information Technology, *Chem. Rev.*, 107, 5082-5100.

Herschbach, D. R. (1987). Molecular Dynamics of Elementary Chemical Reactions, *Angew Chem. Int. Ed. Engl.*, 26, 1221-1243.

Assion, A.; Baumart, T.; Bergt, M.; Brixner, T.; Kiefer, B.; Sayfried, V.; Strehle, M.; Gerber, G. (1998). Control of chemical reactions by feedback-optimized phase-shaped femtosecond laser pulses, *Science*, 282, 919-922.

Daniel, C.; Full, J.; Gonzalez, L.; Kaposta, C.; Krenz, M.; Lupulescu, C.; Manz, J.; Minemoto, S.; Oppel, M.; Rosendo-Francisco, P.; Vajda, Š.; Wöste, L. (2001). Analysis and control on η_5-CpMn(CO)$_3$ fragmentation processes, *Chem. Phys.*, 267, 247-260.

Levis, R. J.; Rabitz, H. A. (2002). Closing the Loop on Bond Selective Chemistry Using Tailored Strong Field Laser Pulses, *J. Phys. Chem. A*, 106, 6427-6444.

Daniel, C.; Full, J.; González, L.; Lupulescu, C.; Manz, J.; Merli, A.; Vajda, S.; and Wöste, L. (2003). Deciphering the reaction dynamics underlying optimal control laser fields, *Science*, 299, 536-539,

Weinacht, T. C.; White, J. L.; and Bucksbaum, P. H. (1999). Towards Strong Field Mode-Selective Chemistry, *J. Phys. Chem. A*, 103, 10166.

Itakura, R.; Yamanouchi, K.; Tanabe, T.; Okamoto, T.; and Kannari, F. (2003). Dissociative ionization of ethanol in chirped intense laser fields. J. Chem. Phys. 119, 4179.

Melinger, J.S.; Gandhi, S.R.; Hariharan, A.; Tull, J.X.; Warren, W.S. (1992). Generation of narrowband inversion with broadband laser pulses, *Phys. Rev. Lett.*, 68, 2000-2003.

Krause, J. L.; Whitnell, R. M.; Wilson, K. R.; Yan, Y.; Mukamel, S. (1993). Optical control of molecular dynamics: Molecular cannons, reflectrons, and wave-packet focusers, *J. Chem. Phys.*, 99, 6562.

Cerullo, G.; Bardeen, C. J.; Wang, Q.; Shank, C. V. (1996). High Power Femtosecond Chirped Pulse Excitation of Molecules in Solution, *Chem. Phys. Lett.* 262, 362-368.

Pastirk, I.; Brown, E. J.; Zhang, Q.; and Dantus, M. (1998). Quantum control of the yield of a chemical reaction, *J. Chem. Phys.*, 108, 4375-4378.

Yakovlev, V. V.; Bardeen, C. J.; Che, J.; Cao, J.; Wilson, K. R. (1998). Chirped pulse enhancement of multiphoton absorption in molecular Iodine, *J. Chem. Phys.*, 108, 2309.

Cao, J.; Che, J.; Wilson, K. R. (1998). Intra-pulse dynamical effects in multi-photon processes: Theoretical analysis, *J. Phys. Chem.*, 102, 4284-4290.

Guilhaus, M. (1995). Principles and instrumentation in time-of-flight mass spectrometry: Physical and instrumental concepts, *J. Mass Spectrometry*, 30, 1519-1532.

Opsal, R. B.; Owens, K. G.; Reilly, J. P. (1985). Resolution in the Linear Time-of-Flight Mass Spectrometer, *Anal. Chem.*, 57, 1884-1889.

Mathur, D.; Rajgara, F. A. (2004). Dissociative ionization of methane by chirped pulses of intense laser light, *J. Chem. Phys.*, 120, 5616.

Lozovoy, V. V.; Dantus, M. (2008). Femtosecond laser-induced molecular sequential fragmentation of para-nitrotoluene, *J. Phys. Chem. A*, 112, 3789-3812.

Goswami, T.; Karthick Kumar, S. K.; Dutta, A.; Goswami, D. (2009). Control of laser induced molecular fragmentation of n-propyl benzene using chirped femtosecond laser pulses, *Chem. Phys.* 360, 47-52.

DeWitt, M. J.; Peters, D. W.; Levis, R. J. (1997). The Photoionization/Dissociation of Alkyl Substituted Benzene Molecules Using Intense Near-Infrared Radiation, *Chem. Phys.* 218, 211-223.

Laser Pulse Phenomena and Applications
Edited by Dr. F. J. Duarte

ISBN 978-953-307-405-4
Hard cover, 474 pages
Publisher InTech
Published online 30, November, 2010
Published in print edition November, 2010

Pulsed lasers are available in the gas, liquid, and the solid state. These lasers are also enormously versatile in their output characteristics yielding emission from very large energy pulses to very high peak-power pulses. Pulsed lasers are equally versatile in their spectral characteristics. This volume includes an impressive array of current research on pulsed laser phenomena and applications. *Laser Pulse Phenomena and Applications* covers a wide range of topics from laser powered orbital launchers, and laser rocket engines, to laser-matter interactions, detector and sensor laser technology, laser ablation, and biological applications.

How to reference
In order to correctly reference this scholarly work, feel free to copy and paste the following:

Debabrata Goswami and Tapas Goswami (2010). Hot Chemistry with Cold Molecules, Laser Pulse Phenomena and Applications, Dr. F. J. Duarte (Ed.), ISBN: 978-953-307-405-4, InTech, Available from: http://www.intechopen.com/books/laser-pulse-phenomena-and-applications/hot-chemistry-with-cold-molecules-

INTECH
open science | open minds

InTech Europe
University Campus STeP Ri
Slavka Krautzeka 83/A
51000 Rijeka, Croatia
Phone: +385 (51) 770 447
Fax: +385 (51) 686 166
www.intechopen.com

InTech China
Unit 405, Office Block, Hotel Equatorial Shanghai
No.65, Yan An Road (West), Shanghai, 200040, China
中国上海市延安西路65号上海国际贵都大饭店办公楼405单元
Phone: +86-21-62489820
Fax: +86-21-62489821

IntechOpen